

THE PERFORMANCE OF SATELLITE RADAR REMOTE SENSING TECHNOLOGY IN GROUND SETTLEMENT MONITORING

Yuxiao Qin¹, Daniele Perissin¹, Matthew Pang¹, Zhiying Wang², Hui Lin¹

1. The Chinese University of Hong Kong
2. Politecnico di Milano, Milan, Italy

ABSTRACT

TerraSAR X-band (TSX) data can provide a high resolution of 1m, short revisit period of 11 days, and sensitive ground subsidence information. Permanent Scatterers (PS) technology was developed as a powerful tool for extracting the ground displacement information from TSX images. In this work, we exploit the potential of TSX for monitoring ground subsiding for the urban area in Hong Kong. A total of 57 TSX images and 11 TanDEM-X (TDX) images acquired between 25th October 2008 and 4th May 2012 were used in the InSAR time series analysis for retrieving subsidence in the study area. A Corner Reflector (CR) validation test is conducted in the area to quantitatively analyze the performance of PS analysis, and the result indicates that the analysis can achieve millimetric accuracy for its monitoring the ground subsidence.

Index Terms— *TerraSAR-X; subsidence monitoring, Hong Kong; InSAR*

1. INTRODUCTION

One of the most important criteria for constructing large-scale man-made features is to monitor severe ground subsiding of adjacent wide area, so a technology is needed that calls for all-time, all-weather and wide-area to monitor ground subsidence. In recent years, Synthetic Aperture Radar Interferometry (InSAR)[1][2] technology have been proved to be a powerful tool that can provide high resolution information on topology and ground displacement[3]. Furthermore, in order to overcome the limitations of InSAR technology, namely the spatiotemporal decorrelation and atmospheric disturbance displacement[4][5], Permanent Scatterers (PSInSAR) technology[6] was proposed. It has been proved that 1 mm accuracy for deformation monitoring can be achieved[7]. Since then, the technology has been applied widely in ground displacement monitoring[8][9][10]. In this study, we studied the ground deformation of the area of interest (AOI) in Hong Kong urban area by means of PSInSAR technology with multi-temporal techniques.

Furthermore, we investigated the accuracy of the technique for ground monitoring. In order to do this, a set of corner reflectors are deployed in our monitoring area, the height will be adjusted manually, and the result will be used for comparing with the result of PS analysis. The PSInSAR analysis applied in this study is implemented by the processing software SARPROZ[11], developed by Daniele Perissin.

2. STUDY AREA

The monitoring area belongs to urban area in Kowloon, Hong Kong. The studied AOI is shown in Figure 1. A total of 57 TerraSAR-X (TSX) images and 11 Tandem-X (TDX) images acquired between the end of 2008 and May 2012 were exploited for the study. The deformation map and Permanent Scatterers were generated and geocoded in SARPROZ[11] and displayed in Google Earth.

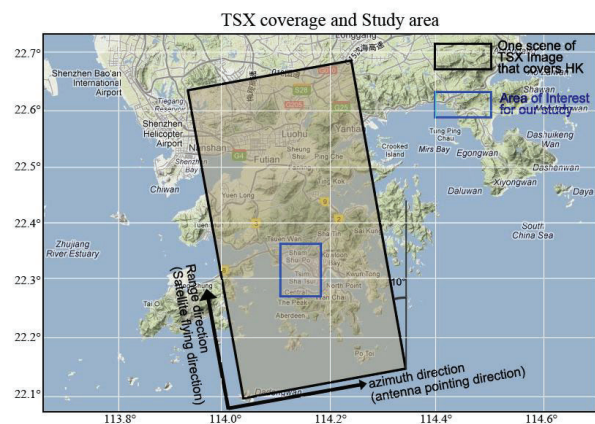


Figure 1. Spatial coverage of TerraSAR-X and our study of interest

3. METHODOLOGY

The case can be divided into two steps: PS analysis and CRs validation test.

3.1. Linear Deformation Map

We firstly choose a reference image known as ‘Master’ of the datasets. In the following analysis, the displacement of the radar targets is retrieved as a function of time with respect to the Master image. The datasets is applied for PSInSAR analysis in SARPROZ. By processing the phase of SAR images with PSInSAR algorithm, two results can be retrieved: the three dimensional localization of Permanent Scatterers (PS’s) with 1m precision, and the estimated millimetric displacement of PS’s along the satellite line of sight. The PS analysis will be updated continuously by adding newly acquired images, and improved by the supplemented CR tests. The final result will be displayed in Google Earth.

3.2. Corner Reflector Test

In order to evaluate the performance of PSInSAR monitoring techniques and the accuracy of ground monitoring results with artificial targets, a set of CRs are deployed in the monitoring region. For the validation test, the CRs are either lifted or lowered manually, and its displacement is recorded by optical leveling. We will then evaluate the accuracy of PSInSAR monitoring by comparing the displacement detected by SAR images and by optical leveling.

3.2.1. Design and Deployment of Corner Reflector

A CR should be easy to point, light to carry, easy to mount, difficult to be reached by unauthorized people, well fixed, resistant to all weather conditions. Additionally, in particular for the experiment we carried out, the height must be adjustable. To meet the above requirements, the CR is designed to be cubic shape and made of aluminum. The side panels are holed. The CR is fixed onto a concrete basement on the ground with four anchors and screws (to fix and adjust its height). The advantage of this type of target is that it does not require any complicated pointing procedure. When deploying the CR, one simply turns the mouth to the satellite viewing direction. A prototype of the CR is shown in Figure 2.

An ideal place for placing CR’s is an area that presents a low background radiation to facilitate identifying the CR and to guarantee good phase stability. In addition, in order to demonstrate the PSInSAR capability of detecting millimetric changes with CR, it is suggested to place all the CR within a certain distance, in order to avoid possible unexpected relative motions and to keep the atmospheric noise as limited as possible. In general, this distance should not exceed 100m. In this experiment, as shown in Figure 3, we deployed four CRs in an area where the background radiation is considerably low. The four CRs are within a range of 200 meters so that the atmospheric noise is kept to a low level. One of them is selected as the reference target for the process, which means it will stay stable for all time.

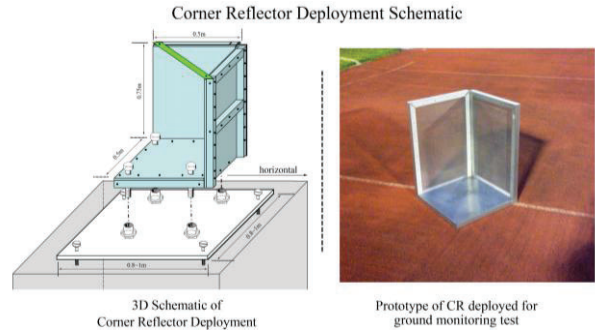


Figure 2. Schematic of Corner Reflector deployment.

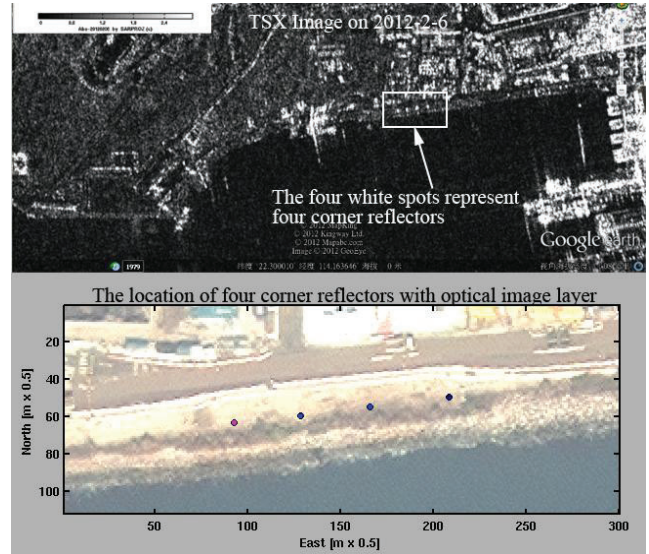


Figure 3 Upper: the location and intensity of the four CRs on TSX images. From the image we can see that the background radiation in that area is very low, and the intensity of CRs is considerably high. Down: the location of CRs geocoded to optical image. The location is near the sea that is identical for its low intensity in RADAR images.

3.2.2. Displacement of Corner Reflector

To estimate the displacement of the CRs, we exploited the intensity of the SAR images and the height measured by the ground survey. Radar images are in fact two-dimensional, and one cannot retrieve the highly accurate height information by analyzing only the intensity of the radar signal.

In this paragraph, we proceed analyzing the phase of the SAR signal reflected by the CRs.

First of all, the interferometric phase can be decomposed into the following terms:

$$\Delta\varphi = \Delta\varphi_{displacement} + \Delta\varphi_{height} + \Delta\varphi_{atmosphere} + \Delta\varphi_{noise} \quad (1)$$

In sequence, the four parameters are possible displacement, height of targets, atmosphere and noise.

The height of a target is usually unknown, and it must be estimated by the PS technique. In our study, the interferometric phase term depending on the relative height

of the CRs is removed by exploiting the height provided by the survey team.

The phase term linked to the atmospheric delay is neglected since the 4 CRs are placed relatively close to each other. The CRs displacement can be retrieved from the interferometric phase exploiting the following equation:

$$\Delta\varphi_{displacement} = \Delta\varphi - \Delta\varphi_{height} - \Delta\varphi_{atmosphere} - \Delta\varphi_{noise} \quad (2)$$

Assuming a low noise level within CRs, one can write:

$$\Delta\varphi_{atmosphere} \approx \Delta\varphi_{noise} \approx 0 \quad (3)$$

So the phase of displacement can be computed as:

$$\Delta\varphi_{displacement} = \Delta\varphi - \Delta\varphi_{height} \quad (4)$$

Where

$$\Delta\varphi = \frac{4\pi}{\lambda} d \quad (5)$$

And

$$d = \frac{\Delta\varphi - \Delta\varphi_{height}}{4\pi} \cong \frac{\Delta\varphi_{displacement}}{4\pi} \quad (6)$$

The displacement retrieved from the interferometric phase is along the Line Of Sight (LOS) of the satellite. The vertical displacement is linked to the LOS displacement d by the following relationship,

$$d = D_{vert} \cos\theta \quad (7)$$

where D_{vert} is the vertical displacement, θ is the inclination angle between the LOS and vertical direction, 37.36 degrees in this case of the TerraSAR-X dataset acquired in Hong Kong. In our dataset, the conversion factor $\cos\theta$ is equal to 0.795.

The displacement retrieved from the interferometric phase is ambiguous. In particular, the following equations hold:

$$\varphi = \varphi \pm 2k\pi \quad (k = 1, 2, 3, \dots) \quad (8)$$

$$d = d \pm k \frac{\lambda}{2} \quad (k = 1, 2, 3, \dots) \quad (9)$$

For the TerraSAR-X, the wavelength λ equal to 3.1cm, the displacement retrieved from the interferometric phase will be

$$d = d \pm k15.5mm \quad (k = 1, 2, 3, \dots) \quad (10)$$

Given the theoretical framework, we can then approach the real data of our case study.

4. RESULTS

4.1. Linear Deformation Map

Figure 4 shows the linear deformation map (corresponding to the average displacement trend) obtained by processing the dataset with the PSInSAR technique. From the figure we can read the values ranging from about 0 to -15mm/year. The west part of monitoring area shows an obvious trend of subsidence with a velocity of 0 to 5mm/year.

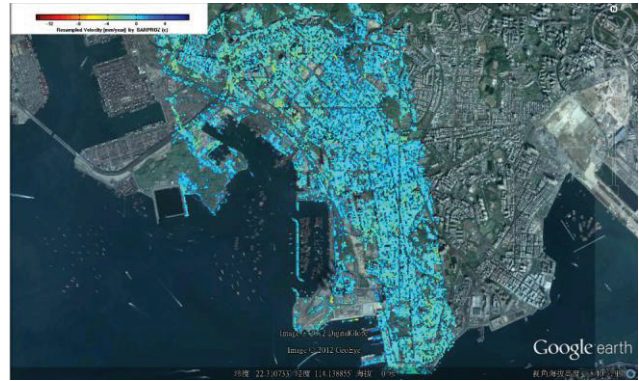


Figure 4. Linear Displacement Map for PSs that have a height within the region of [-5,5] meters.

Figure 5 shows a three dimensional representation of the PS location in Google Earth. The target shown is located at ground level along the coast, at ground level (height close to zero) and it shows clearly a linear displacement of the whole terrain on the selected PS: -13.4mm/year. The deformation trend on 4th May 2012 is -19mm, confirming the subsiding trend over the area.

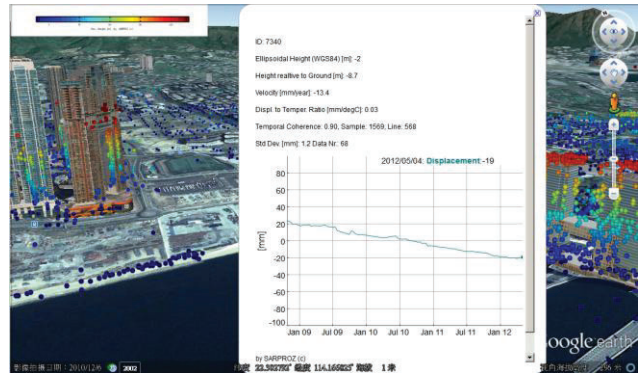


Figure 5. An example of one PS point located in our AOI.

4.2. Displacement of Corner Reflector and Deviation

After the corner reflectors were being deployed, a series of test were conducted, and we can retrieve the results obtained from SAR images and ground survey. The result is listed out in Table 1.

Date of Satellite Images	Vertical displacement by SAR images (mm)				Vertical displacement Surveyed (mm)			
	No.1	No.2	No.3	No.4	No.1	No.2	No.3	No.4
06/Feb/12	0	0	0	0	0	0	0	0
17/Feb/12	8.4	8.9	4.4	0	10	10	5	0
21/Mar/12	-5.2	19.6	9.6	0	-5	19	8	0
01/Apr/12	-5.7	18.8	5.6	0	-5	18	5	0
12/Apr/12	-0.3	26.9	-0.2	0	-1	26	-1	0
23/Apr/12	2.1	19.3	8.5	0	3	20	8	0

Table 1. The comparison of vertical displacements between SAR images results and surveyed results. CR No.4 is the reference CR thus it is not moved.

Comparing the result from SAR images and optical leveling, we can see that the numbers are really close, and for most cases the deviation is less than 1mm. To analyze the

deviation between the two measurements, a linear regression is conducted, and the result is shown in Figure 6. For each target in this figure, the x-axis value indicates the vertical displacement measured by the optical survey, and the y-axis value indicates the vertical displacement detected by SAR images. The outcome of the linear regression is

$$y = 1.0159x - 0.08043 \quad (11)$$

Since the ideal model for the case should be $y = x$, thus the above equation (11) means a bias of less than a tenth of millimeter and a deviation from the linear relation of about 1%.

In addition, the correlation coefficient R^2 is equal to 0.9909, stating univocally the linear correlation between the displacement detected by InSAR and by the optical survey. The root mean square error (RMSE) has a value of 0.94 mm, slightly lower than 1mm, which is the theoretical accuracy of optical leveling. In other words, the outcome of the analysis is slightly better than the best result that could be expected from such an analysis, revealing that InSAR can definitely reach the same accuracy of optical leveling, and maybe overtake it.

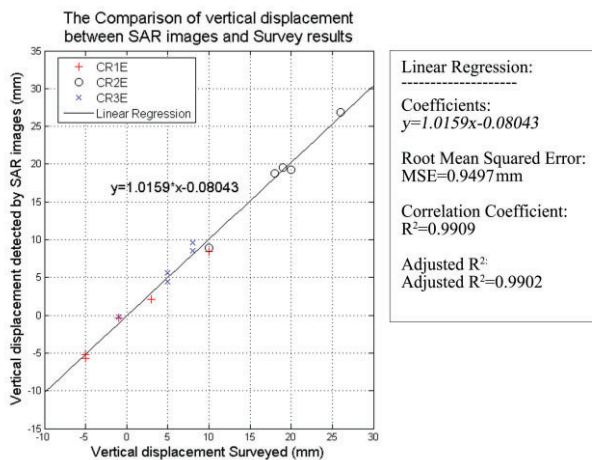


Figure 6. A statistical analyses on the deviation between the displacement detected by InSAR and by optical leveling measurement.

5. CONCLUSION

In this paper, we analyzed the ground deformation trend in Hong Kong West Kowloon urban area. The result shows clearly the local ground subsiding of about 5mm/year. To further validate the accuracy of the PS analysis, a corner reflector test is conducted inside our AOL. The results showed a very high coefficient between the displacement between the InSAR analysis and the ground survey result and a deviation of less than 1mm. The method is definitely showing the capability of achieving the same level of ground survey, meanwhile much more convenient than conducting ground survey in monitoring ground subsidence.

5. ACKNOWLEDGEMENT

The TerraSAR-X data used in this project have been provided by Infoterra Germany, through the cooperation with Ralf Duering, Beijing. This work was partially supported by the Research Grants Council (RGC) General Research Fund (GRF) (Proj. Ref. No.415911) of HKSAR.

REFERENCES

- [1] J. C. Curlander, R. N. McDonough, "Synthetic Aperture Radar: Systems and Signal Processing", New York, John Wiley & Sons, 1991
- [2] R. Gens, J. L. Van Genderen, "SAR Interferometry - Issues, Techniques, Applications", International Journal of Remote Sensing, 17, 1803-1835.
- [3] F. Amelung, D.L. Galloway, J.W. Bell, H.A. Zebker, R.J. Laczniaik, "Sensing the ups and downs of Las Vegas: InSAR reveals structural control of land subsidence and aquifer-system deformation", Geology, 27 (1999), pp. 483-486.
- [4] Zebker, H.A. and J. Villaseñor, "Decorrelation in interferometric radar echoes". IEEE Transactions on Geoscience and Remote Sensing, 1992. 30(5): p. 950-959.
- [5] Zebker, H.A. and P. Rosen, "Atmospheric artifacts in interferometric SAR surface deformation and topographic maps". J. Geophys. Res. Solid Earth, 1997. 102(4): p. 7547-7563.
- [6] A. Ferretti, C. Prati and F. Rocca, "Permanent Scatterers in SAR Interferometry", IEEE TGARS, Vol. 39, no. 1, 2001.
- [7] Ferretti, A., et al., "Submillimeter accuracy of InSAR time series: Experimental validation". IEEE Transactions on Geoscience and Remote Sensing, 2007. 45(5): p. 1142-1153.
- [8] Alex Hay-Man Ng, L. Ge, X. Li and K. Zhang, "Monitoring ground deformation in Beijing, China with persistent scatterer SAR interferometry", Journal of Geodesy, Volume 86, Number 6 (2012), 375-392.
- [9] Q. Zhao, et al., "InSAR detection of residual settlement of an ocean reclamation engineering project: a case study of Hong Kong International Airport". Journal of Oceanography, Volume 67, Number 4 (2011), 415-426.
- [10] G. Herreraa, et al., "Validation and comparison of Advanced Differential Interferometry Techniques: Murcia metropolitan area case study". ISPRS Journal of Photogrammetry and Remote Sensing, Volume 64, Issue 5, September 2009, Pages 501-512.
- [11] SARPROZ software manual: <http://ihome.cuhk.edu.hk/~b122066/manual/index.html>